23rd ABCM International Congress of Mechanical Engineering
December 6-11, 2015, Rio de Janeiro, RJ, Brazil

HYDRATE FILM GROWTH MODEL - MASS AND ENERGY TRANSPORT FOR METHANE AND CARBON DIOXIDE HYDRATES

Luiz Henrique Accorsi Gans
Guilherme Mühlstedt
Paulo Henrique Dias dos Santos
Moisés Alves Marcelino Neto
Rigoberto Eleazar Melgarejo Morales
Multiphase Flow Center (NUEM), Postgraduated Program in Mechanical and Materials Engineering (PPGEM), Federal Technological University of Paraná (UTFPR) – Av. Sete de Setembro, 3165 - Rebouças CEP 80230-901 - Curitiba - PR – Brasil
luizgans@gmail.com, tedt49@gmail.com, paulosantos@labcet.ufsc.br, mneto@utfpr.edu.br, rmorales@utfpr.edu.br

Amadeu K. Sum
Center for Hydrate Research, Department of Chemical & Biological Engineering, Colorado School of Mines, 1500 Illinois St, Golden, CO 80401, USA.
asum@mines.edu

Abstract. *The study of clathrate-hydrate formation processes in pipelines is very important to the oil and gas industry because these structures can stop production and represent a safety risk due to the pressure build-up in the pipelines. Several research groups have proposed different models to predict how a hydrate film grows. However, the models based only on heat transfer could not explain satisfactorily the experimental data because gas consumption was disregarded. So, in order to clarify the deposition phenomenon, the current work presents a mathematical model for the uncoupled mass and energy balance problem for CO_2 and CH_4 hydrates.*

Keywords: *CO_2 and CH_4 Hydrates, Film Growth, Mathematical Modeling, Heat and Mass Transfer.*

1. INTRODUCTION

The number of gas hydrate-related publications has been increasing every year, showing the important applications of gas hydrate in many fields, including flow assurance of oil and gas pipelines, natural energy resource from deep-sea and permafrost hydrate deposits, CO_2 sequestration in deep ocean, transportation of natural gas, gas separation, seawater distillation and others (Sloan and Koh, 2008).

In recent years important oil reserves have been found in deep sea. Gas hydrates in deepwater flowlines are more likely to occur because of its high pressure and low temperature conditions. Their presence may stop the oil and gas production by forming a plug and they also represent a safety risk to the pipeline, platform and crew if there is a pressure build-up, since the plug can behave as projectiles (Sloan, 2000). Thus, in order to avoid unpredictable costs and assure the flow in the pipeline, it is highly desirable and critical to understand how hydrates form and grow.

Gas hydrates are crystalline compounds formed by water molecules that are hydrogen-bonded to each other with an oxygen at each vertex and a guest molecule (approximately 85 mol% water, 15 mol% guest molecules) (Sloan and Koh, 2008). In the oil and gas industry, carbon dioxide and methane represent two of the main guest gases during operations, so several research groups have tried to formulate a model capable to describe how these hydrates form and grow (Uchida et al., 1999; Freer et al., 2001; Mori, 2001; Mori and Mochizuki, 2006). Most part of these studies conceived a mathematical or numerical model based on heat transfer equations. However, to the present day no mathematical model has been able to predict how the hydrate grows.

Kelkar et al. (1998) and Peters et al. (2000) had already formulated and validated numerical models for hydrate dissociation using only the energy balance. But the hydrate formation and growth must also be related with the gas consumption.

Therefore, it has been pointed that hydrate growth is mass transfer dependent, where gas consumption is an important variable and it should be observed in the hydrate growth model (Englezos et al, 1987; Vysniaukas and Bishnoi, 1983).

As no consistent model has been presented for hydrate growth, the current paper aims to offer a simplified overview of this problem, considering uncoupled heat and mass transfer problems. This way, it is expected to understand how important both heat and mass transfers are in order to better describe and represent that phenomenon.

2. HEAT AND MASS TRANSFER THEORY

Given that methane and carbon dioxide represent two high concentration gases in an offshore oil extraction, both gas hydrates will be modeled in two pure gas-saturated water systems. In a real system, these gases exit the well-head mixed in the oil and water phases in a high temperature. As they flow, the ocean cools the fluids throughout the pipe wall allowing the hydrate formation when they reach the hydrate envelope. Along the pipeline, hydrate clusters can also nucleate between two different phases and agglomerate until the blockage of the pipe. However, this work studies only the wall hydrate deposition from a pure gas-saturated water system.

After the first hydrate layer has been fixed on the wall, it will grow while its interface is within the hydrate thermodynamic formation region and gas is being consumed from the aqueous phase.

Figure 1 represents the hydrate growth in a pipeline for a gas-saturated water flow. It also shows the pipe inner diameter (D_i), the hydrate thickness (δ) and its boundary conditions.

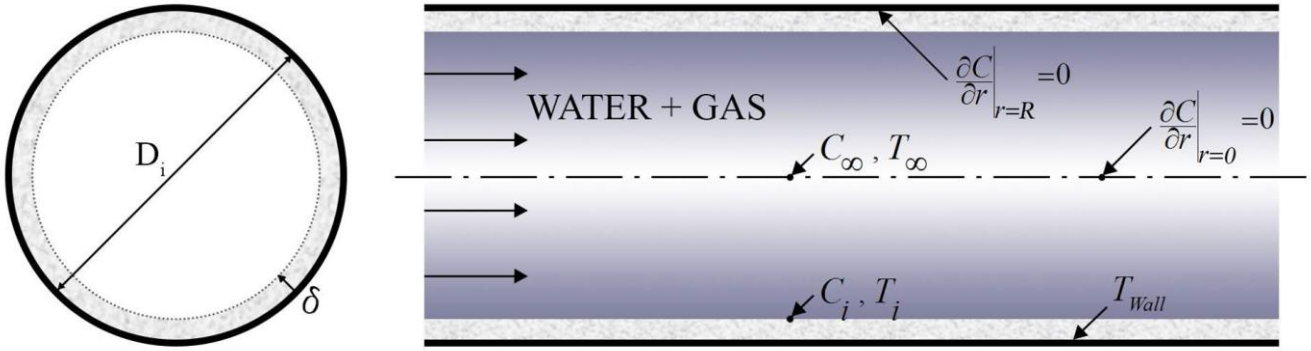

Figure 1 – Gas-saturated water flow in a pipeline.

Due to the flow complexity, it has been decided to simplify the model by neglecting the fluid velocity component. This way, analytical solutions could be developed.

As the hydrate grows radially from the wall, the problem can be simplified to a unidimensional perspective. Further, in the very first hours the hydrate thickness is much smaller than the pipe curvature, so Cartesian coordinates were assumed, as demonstrated in Figure 2.

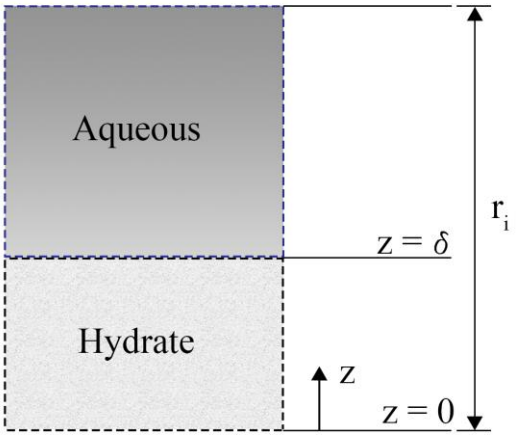

Figure 2 – One-dimensional hydrate growth.

Where r_i indicates the pipe inner radius and δ the instantaneous hydrate thickness.

2.1 Heat Transfer

Considering that there is no flow in the hydrate or in the aqueous phase and that the hydrate comes up from a heterogeneous reaction (superficial phenomenon), advective terms and reaction are neglected in the governing equations. The hydrate porosity is assumed constant. So, the hydrate growth depends only on the diffusive terms and on the phase change through time, as follow:

Hydrate phase

$$\frac{\partial^2 T_h}{\partial z^2} = \frac{1}{\alpha_h}\frac{\partial T_h}{\partial t} \qquad \text{for } 0 < z < s(t),\ t > 0 \tag{1}$$

$$T_h(z,t) = T_{wall} \qquad \text{at } z = 0,\ t > 0 \tag{2}$$

Where α_h represents the hydrate diffusivity and T_{wall} the wall temperature.

Aqueous phase

$$\frac{\partial^2 T_w}{\partial z^2} = \frac{1}{\alpha_w}\frac{\partial T_w}{\partial t} \qquad \text{for } \delta < z < \infty,\ t > 0 \tag{3}$$

$$T_w(z,t) = T_0 \qquad \text{for } t = 0,\ z > 0 \tag{4}$$

$$T_w(z,t) \to T_0 \qquad \text{at } z \to \infty,\ t > 0 \tag{5}$$

Where α_w represents the gas-saturated water diffusivity and T_0 the initial temperature.

The coupling between hydrate and aqueous phase is done with an energy balance at the interface:

$$T_h(z,t) = T_w(z,t) = T_i \qquad \text{at } z = \delta(t),\ t > 0 \tag{6}$$

$$k_h\frac{\partial T_h}{\partial z} - k_w\frac{\partial T_w}{\partial z} = (1-\varepsilon)\rho_h \Delta H_F \frac{d\delta}{dt} \qquad \text{at } z = \delta, t > 0 \tag{7}$$

Where k_h is the hydrate conductivity, k_w the water conductivity, ε the porosity, ρ_h the hydrate density and ΔH_F the hydrate formation enthalpy. Equation (7) is very important because it relates how the phase change heat is removed from the system. This equation also represents an energy balance at the hydrate interface and, in this case, it considers that the phase change heat is removed exclusively by conduction.

The previous equations show a well-known analytical solution which is presented below. The temperature profile solutions for both hydrate and aqueous phase are given by Eqs. (8) and (9).

$$T_h(z,t) = T_{wall} + A \cdot erf\left[z / 2(a_h t)^{1/2}\right] \tag{8}$$

$$T_w(z,t) = T_0 + B \cdot erf\left[z / 2(a_w t)^{1/2}\right] \tag{9}$$

Where A and B are constants. When z= δ , T_h and T_w are equal to the interface temperature.

$$T_{wall} + A \cdot erf(\lambda) = T_0 + B \cdot erfc\left[\lambda\left(\frac{\alpha_h}{\alpha_w}\right)^{1/2}\right] = T_i \tag{10}$$

Where:

$$\lambda = \frac{\delta}{2(\alpha_w t)^{1/2}} \qquad \text{or} \qquad \delta = 2\lambda(\alpha_w t)^{1/2} \tag{11}$$

$$A = \frac{T_i - T_{parede}}{erf(\lambda)}, \quad B = \frac{T_i - T_0}{erfc\left[\lambda(\alpha_h / \alpha_w)^{1/2}\right]} \tag{12}$$

Replacing the constants from the Eq. (12) onto the Eqs. (8) and (9), the final solution is found. Thickness and profile temperatures are time dependent and all the physical properties are related to the parameter λ which is the solution for the transcendental equation shown in Eq. (16).

$$\delta(t) = \lambda.2(\alpha_h t)^{1/2} \tag{13}$$

$$\frac{T_h(z,t)-T_{wall}}{T_i-T_{wall}} = \frac{erf\left[\mathrm{z}/\,2\left(\alpha_h t\right)^{1/2}\right]}{erf\left(\lambda\right)} \tag{14}$$

$$\frac{T_w(z,t)-T_0}{T_i-T_0} = \frac{erfc\left[\mathrm{z}/\,2\left(\alpha_w t\right)^{1/2}\right]}{erfc\left[\lambda\left(\alpha_h/\alpha_w\right)^{1/2}\right]} \tag{15}$$

$$\frac{e^{-\lambda^2}}{erf\left(\lambda\right)} + \frac{k_w}{k_h}\left(\frac{\alpha_h}{\alpha_w}\right)^{1/2}\frac{\left(T_i-T_0\right)}{\left(T_i-T_{wall}\right)}\frac{e^{-\lambda^2(\alpha_h/\alpha_w)}}{erfc\left[\lambda\left(\alpha_h/\alpha_w\right)^{1/2}\right]} = \frac{\left(1-\varepsilon\right)\Delta H_F\lambda\sqrt{\pi}}{c_{p,h}\left(T_i-T_{wall}\right)} \tag{16}$$

2.2 Mass Transfer

Mass transfer is expressed by the consumption of the gas presented in the aqueous phase which is converted into hydrate at the solid-liquid interface, as it is shown in Figure 2. So, applying the same assumptions used for heat transfer, it is possible to raise the concentration profile over time in the liquid phase. The symmetry condition in the center of the pipe and the concentration value at the interface are represented by Eq. (18) and Eq. (19), respectively. The initial condition is shown by Eq. (20).

$$D_{gw}\frac{\partial^2 C}{\partial \mathrm{z}^2} = \frac{\partial C}{\partial t} \tag{17}$$

Where D_{gw} is the mass diffusion coefficient for the gas in the aqueous phase.

Boundary conditions

$$\left.\frac{\partial C_g}{\partial \mathrm{z}}\right|_{z=r_i} = 0 \qquad t \geq 0 \tag{18}$$

$$C_g\left(z=\delta,\mathrm{t}\right) = C_{\mathrm{g},i} \qquad \text{para}\, t>0 \tag{19}$$

Initial condition

$$C\left(z,0\right) = C_\infty \qquad \text{at}\;\; t=0 \tag{20}$$

This time dependent problem with these boundary and initial conditions is solved by separation of variables and it presents a well-known solution, shown by Eq. (21).

$$\frac{C-C_{\mathrm{g},i}}{C_{\mathrm{g},\infty}-C_{\mathrm{g},i}} = \sum_{n=1}^{\infty}\frac{4\,\mathrm{e}^{\frac{-(2n-1)^2\pi^2 D_{gw}t}{4(r_i-\delta)^2}}}{\pi\left(2n-1\right)}\sin\left[\frac{\left(2n-1\right)\pi\left(z-\delta\right)}{2\left(r_i-\delta\right)}\right] \tag{21}$$

2.3 Physical Properties

All the physical properties for both hydrate and liquid phases are result of an extensive research. Data were collected from several papers and from the softwares CSMGem and Multiflash. The reference pressure for hydrate formation was set to 100 bar (10.000 kPa) and the pipeline inner radius was 4 inches (101.6 mm).

Usually the hydrate porosity is higher in the early stages and decreases drastically over time (Sloan and Koh, 2008). That is why it was decided to set an average value of 50% to the porosity.

Table 1 – Physical Properties

Symbol	Properties	Units	CO_2 Hydrate	CH_4 Hydrate	CO_2 + H_2O (l)	CH_4 + H_2O (l)
P	Pressure	bar	100			
ρ	Density	kg/m³	1105 [a]	917 [a]	1048 [a]	1003 [a]
ε	Porosity	-	0.5	0.5	Not applicable	
C_p	Specific heat	J/kg.K	2051 [e]	2250 [f]	4208 [d]	4208 [d]
M	Molar weight	g/mol	21.583 [a]	17.731 [a]	18.808 [a]	18.011 [a]
ΔH_F	Latent heat	J/mol	60000 [f]	53000 [f]	Not applicable	
k	Thermal conductivity	W/m.k	0.49 [g]	0.49 [g]	0.574 [d]	0.574 [d]
D	Diffusion coefficient	m²/s	1.00E-12 [f]	5.00E-13 [i]	1.36E-09 [j]	8.50E-10 [k]
α	Thermal diffusivity	m²/s	2.16E-07 [c]	3.10E-07 [l]	1.30159E-07 [c]	1.35999E-07 [c]
T_∞	Bulk temperature	K	Not applicable		288.64	291
T_i	Interface temperature	K	283.641 [a]	286.06 [a]	Not applicable	
T_{wall}	Wall temperature	K	277			
n	Hydration number	-	5.75 [c]	5.75 [c]	Not applicable	
$C_{g,i}$	Interface concentration	mol/kg	0.76 [f/m]	0.116 [f]	Not applicable	
$C_{g,\infty}$	Bulk concentration	mol/kg	Not applicable		1.62 [b]	0.123 [b]
r_i	Pipeline inner radius	pol//mm	4 // 101.6			

[a] CSMGem, [b] Multiflash, [c] Theoretical, [d] Incropera (water data), [e] Mochizuki e Mori (2006), [f] Jung et al (2010), [g] Sloan e Koh (2007), [i] Davies et al. (2008), [j] Frank et al. (1996), [k] Witherspoon e Bonoli (1969), [l] Waite et al. (2007), [m] Extrapolated values

3. RESULTS AND DISCUSSIONS

Given the properties for methane and carbon dioxide systems, the parameter λ in Eq. (11) is equal to 0.228 and 0.197, respectively. With this, the hydrate thickness and the temperature profile for both hydrate and aqueous phase were calculated, which is shown in Figs. 3 and 4 respectively.

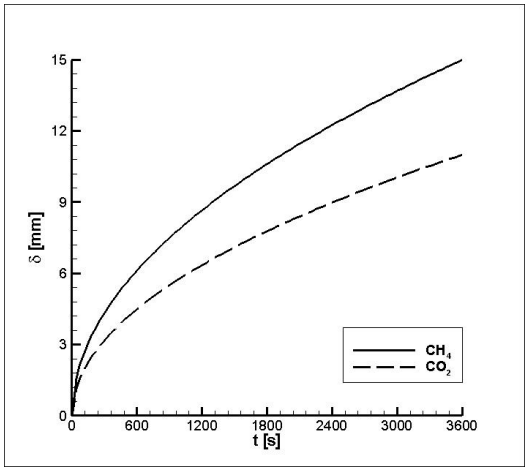

Figure 3 – Thickness over time for methane and carbon dioxide hydrates.

In Fig. 3 the hydrate thickness considers only the energy balance with phase change. Methane hydrate grows faster than the carbon dioxide hydrate, as predicted by the literature (Uchida et al., 1999 and Freer et al., 2001). After 1h, the hydrate thickness has 15.21 mm and 10.99 mm for methane and carbon dioxide systems, respectively.

The hydrate front velocity decreases over time and it can be calculated by the curve inclination in Fig. 3. Extrapolating the curvature hypothesis, it is possible to estimate an average speed considering the time needed to block the entire pipeline with hydrate. Thereat, the average speed for both hydrate fronts is shown below in Tab. 2.

Table 2 – Hydrate average front speed

Gas Hydrate type	CO_2	CH_4
Average Speed ($\overline{V}$) [μm/s]	0.330	0.632
Blocking time [days]	3.56	1.86

The temperature profile for both phases can be seen in Fig. 4. Arrows indicate the hydrate front for a given time and the z axis represents the domain from the wall to the center of the pipe. The proximity of the temperature profile to a straight line in the hydrate phase is due to low values of the parameter λ .

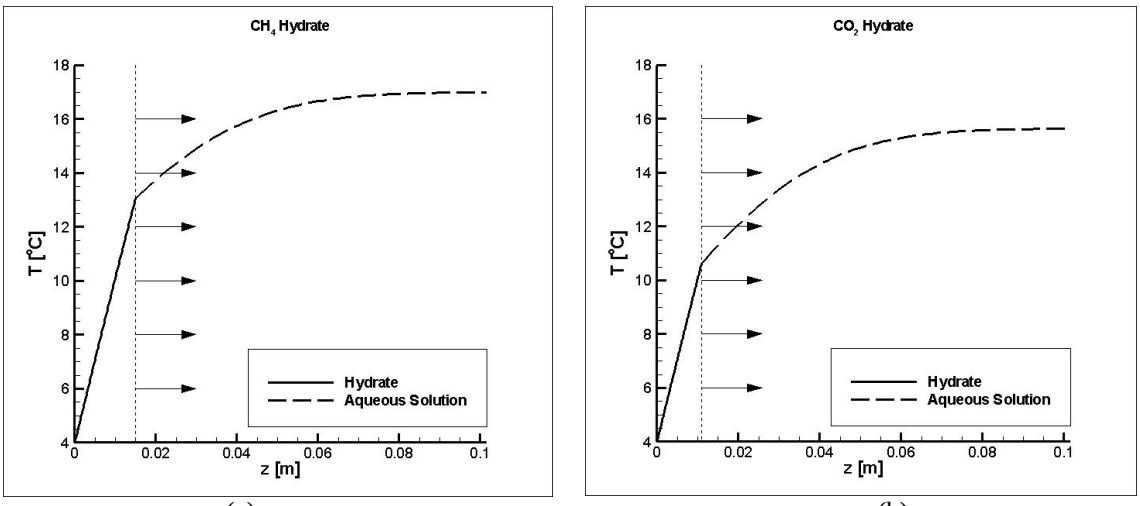

(a) (b)

Figure 4 – Temperature profiles for t=1h after the first hydrate crystals were formed.

In this scenario, considering the hydrate front fixed after 1h of phase change, the concentration profiles in the aqueous phase are presented in Figure 5, where the z axis begins at the hydrate front and finish at the center of the pipe. Theses curves indicate how fast the gas is consumed from the aqueous phase and how long it would take to uniform the concentration over the aqueous domain, indicating a full occupancy of hydrate in the pipe.

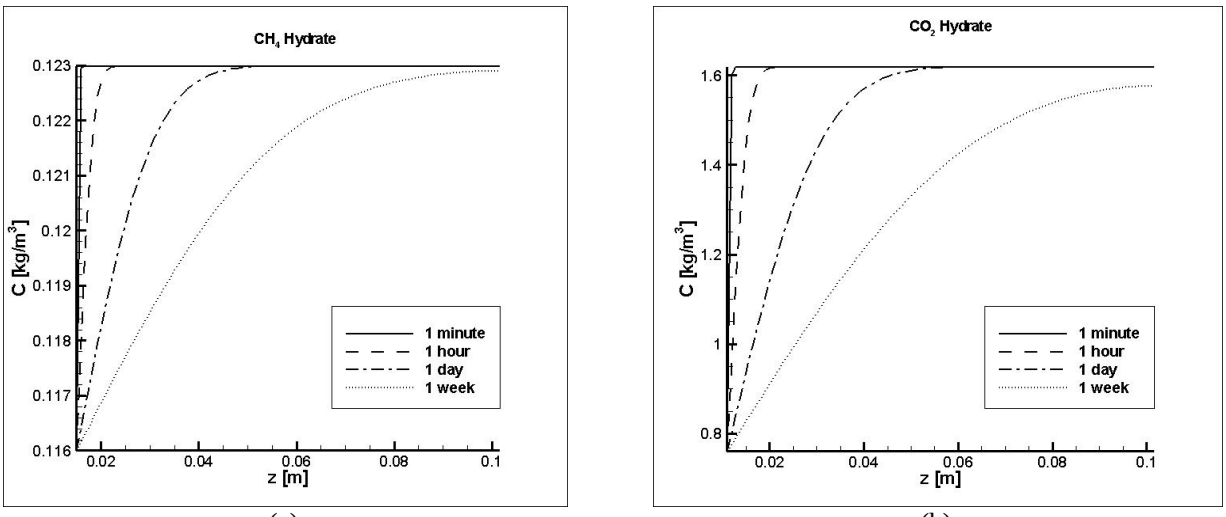

(a) (b)

Figure 5 – Concentration profiles over time.

It can be observed in Figure 5 (a) and (b) that the concentration gradient takes a long time to smooth out. They also suggest that the hydrate would take more than a week to block the pipe. This time is much longer than the calculated heat transfer model time. So, comparing them, it is likely that the mass transfer presents a very important role in the hydrate growth phenomenon and it should decrease the hydrate front velocity.

4. CONCLUSIONS

In this paper it was investigated the methane and carbon dioxide hydrate deposition on the surface of a pipeline. In order to understand how important heat and mass transfer are, both balance equations were analyzed separately for two pure gas-saturated water systems.

By the energy balance analysis, methane hydrate grows faster than carbon dioxide hydrate and their thickness reach 15.21 mm and 10.99 mm, respectively, in the first hour. Although, the presence of gas is imperative to the hydrate formation, so the mass transfer should be also considered in the hydrate growth model. The gas consumption is represented by the concentration gradient in the aqueous phase.

The mass transfer model showed that the gas consumption decreases over time. It was also observed that the hydrate layer would take much longer to match to the heat transfer thickness. This might suggest that the mass balance should reduce the hydrate front velocity. Therefore, in order to achieve more realistic results, both balance equations should be analyzed together in a coupled problem. This coupling might be done at the interface condition, relating the phase change with the gas consumption rate and the heat removal.

For further studies, the use of cylindrical coordinates would also be interesting since it is desired to estimate how long it would take to fulfill the pipeline with hydrate.

5. ACKNOWLEDGEMENTS

The authors acknowledge the financial support from ANP and FINEP through the Human Resources Program to oil and gas segment PRH-ANP (PRH 10 – UTFPR), from REPSOL/SINOPEC and also from the National Scientific and Technological Development Council (CNPq).

6. REFERENCES

Bird, R.B., Stewart, W.E., Lightfoot, E.N., 2004. *Fenômenos de transporte.* University of Wisconsin-Madison: LTC – Livros Técnicos e Científicos Editora S.A., 2ª Edição.

Davies, S. R., J. W. Lachance, E. D. Sloan, and C. A. Koh, 2008. "A novel approach to measuring methane diffusivity through a hydrate film using differential scanning calorimetry". In 6th International Conference on Gas Hydrates. Vancouver, B. C., Canada.

Davies, Simon R., 2009. "The role of transport resistances in the formation and remediation of hydrate plugs". PhD Thesis, Colorado School of Mines, Colorado, IL, USA.

Englezos, P., Kalogerakis, N., Dholabhai, P.D., Bishnoi, P.R., 1987. "Kinetics of formation of methane and ethane gas hydrates". Chemical Engineering Science, Vol. 42, No. 11, pp. 2647-2658.

Esben, E.K., Østergaard, K.K., Tohidi, B., 2002. "A Quasi Steady-State Model for the Dissociation of Gas Hydrates in Pipelines". In Fourth International Conference on Gas Hydrates, Yokohama, May 19-23.

Forsdyke, I., 2000. "Integrated Flow Assurance Overview and Strategy Report". DeepStar Report CTR 4211–1.

Frank, M.J.W., Kuipers, J.A.M, Swaaij, W.P.M., 1996. "Diffusion coefficients and viscosities of CO2 + H2O, CO2 + CH3OH, NH3 + H2O, and NH3 + CH3OH liquid mixtures". Journal of Chemical & Engineering Data, Vol. 41, pp. 297-302.

Freer, E.M., Selim, M.S., Sloan, E.D., 2001. "Methane hydrate film growth kinetics". Fluid Phase Equilibria, Vol. 185, pp. 65-75.

Hong, D.N, Gruy, F., Herri, J.M., 2006. "Experimental data and approximate estimation for dissociation time of hydrate plugs". Chemical Engineering Science, Vol. 61, pp. 1846-1853.

Incropera, F.W.; DeWitt, D. P., 2008. *Fundamentos de Transferência de Calor e de Massa*. Rio de Janeiro: LTC – Livros Técnicos e Científicos Editora S.A.

Jung, J.W., Espinoza, D.N., Santamarina, J.C., 2010. "Properties and phenomena relevant to CH4 – CO2 replacement in hydrate – bearing sediments". Journal of Geophysical Research, Vol. 115, B10102.

Kelkar, S.K., Selim, M.S., Sloan, E.D., 1998. "Hydrate dissociation rates in pipelines". Fluid Phase Equilibria, Vol. 150-151, pp. 371-382.

Mochizuki, T., Mori, Y.H., 2006. "Clathrate-hydrate film growth along water/hydrate-former phase boundaries-numerical heat-transfer study". Journal of Crystal Growth, Vol. 290, pp. 642-652.

Mori, Y.H., 2001. "Estimating the thickness of hydrate filmes from their lateral growth rates: application of a simplified heat transfer model". Journal of Crystal Growth, Vol. 223, pp. 206-212.

Özisik, M. N., 1993. *Heat Conduction*. North Carolina State University: John Wiley & Sons, INC, Second Edition.

Peters, D., Selim, M.S., Sloan, E.D., 2000. "Hydrate dissociation in pipeliness by two-sided depressurization: Experiment and Model". Gas Hydrates Challenges for the Future, Annals of the New York Academy of Sciences, New York, vol. 912, pp. 304–313.

Sloan, E.D., 2000. *Hydrate Engineering***.** Monograph. Richardson, Texas.

Sloan ED, 2003. "Fundamental principles and applications of natural gas hydrates". *Nature*, 426:353–359

Sloan, E.D.; Koh, C.A., 2008. *Clathrate Hydrates of Natural Gases*. 3ª Edição, Flórida, E.U.A.: Editora CRC Press.

Sloan, E.D. et al., 2011. *Natural Gas Hydrates in Flow Assurance*. Burlington, E.U.A.: Editora GPP.

Uchida, T., Ebinuma, T., Kawabata, J., Narita, H., 1999. "Microscopic observations of formation processes of clathrate-hydrate filmes at na interface between water and carbon dioxide". Journal of Crystal Growth, Vol. 204, pp. 348-356.

Vysniaukas, A., Bishnoi, P.R., 1983. "A kinetic study of methane hydrate formation". Chemical Engineering Science, Vol. 38, No 7, pp. 1061-1972.

Waite, W.F. et al., 2009. "Physical properties of hydrate-bearing sediments". *Rev. Geophys.*, 47, RG4003.

Witherspoon, P.A., Bonoli, L., 1969. "Correlation of diffusion coefficients for paraffin, aromatic, and cycloparaffin hydrocarbons in water". Ind. Eng. Chem. Fundam., 8(3), 589–591.

7. RESPONSIBILITY NOTICE

The authors are the only responsible for the printed material included in this paper.